HHS Public Access

Author manuscript

Anesth Analg. Author manuscript; available in PMC 2020 November 01.

Published in final edited form as:

Anesth Analg. 2019 November ; 129(5): 1273–1280. doi:10.1213/ANE.0000000000003572.

Comparison of Broadband and Discrete Wavelength Near Infrared Spectroscopy Algorithms for the Detection of Cytochrome aa_3 Reduction

Robert H. Thiele, M.D. [Associate Professor], **Keita Ikeda, Ph.D. [Principal Scientist]**, **Hari P. Osuru, Ph.D. [Research Scientist]**, **Zhiyi Zuo, M.D., Ph.D. [Professor]**

Department of Anesthesiology, University of Virginia School of Medicine

Abstract

Background: Cytochrome aa_3, the terminal component of the electron transport chain, absorbs near infrare radiation differentially depending on its oxidation state (Cyt_{ox}), which can in theory be measured using near infrared spectroscopy (NIRS) by relating light absorption at specific wavelengths to chromophore concentrations. Some NIRS algorithms use discrete wavelengths, while others analyze a band of NIR (broadband NIRS). The purpose of this study was to test the reproducibility of a discrete wavelength and broadband algorithms to measure changes in Cyt_{ox} (primary outcome), and to determine whether or not a discreet wavelength NIRS algorithm could perform similarly to a broadband NIRS algorithm for the measurement of Cyt_{ox} in a staged hypoxia-cyanide model (hypoxia and cyanide have oppositional effects on tissue saturation, but both cause cytochrome reduction).

Methods: 20 Sprague-Dawley rats were anesthetized with isoflurane, intubated, and instrumented. Blood pressure, end-tidal CO_2, and arterial oxygen saturation (SpO_2) were measured. A halogen light source transmitted NIR transcranially. NIR from the light source and the skull was transmitted to two cooled CCD spectrometers. Rats were subjected to anoxia (FiO_2 0.0) until SpO_2 decreased to 70%. After recovery, 5 mg/kg sodium cyanide was injected intravenously. The cycle was repeated until cardiac arrest occurred. Relative concentrations of hemoglobin and cytochrome aa_3 were calculated using discreet wavelength and broadband NIRS algorithms.

Results: Hypoxia led to an increase in calculated de-oxyhemoglobin (0.20 arbitrary units [AU], 95% CI 0.17 to 0.22, $p < 0.0001$), a decrease in calculated oxy-hemoglobin (−0.16 AU, −0.19 to −0.14, $p < 0.0001$), and a decrease in calculated Cyt_{ox} (−0.057 AU, −0.073 to 0.0040, $p < 0.001$). Cyanide led to a decrease in calculated de-oxyhemoglobin (−0.037 AU, 95% CI −0.046 to −0.029, $p < 0.001$), an increase in calculated oxy-hemoglobin (0.053 AU, 0.040 to 0.065, $p < 0.001$), and a

Corresponding Author: Robert H. Thiele, M.D., Department of Anesthesiology, University of Virginia, PO Box 800710-0710, (434) 243-9412, (434) 982-0018, rht7w@virginia.edu.

Contribution: Robert H. Thiele M.D.: study design, analysis and interpretation of data, manuscript preparation; Keita Ikeda Ph.D.: conduct of study, analysis and interpretation of data, manuscript preparation; Hari P. Osuru Ph.D.: conduct of study, analysis and interpretation of data, manuscript preparation; Zhiyi Zuo M.D., Ph.D.: study design, analysis and interpretation of data, manuscript preparation

Attestation: Robert H. Thiele approved the final manuscript. Robert H. Thiele attests to the integrity of the original data and the analysis reported in this manuscript. Robert H. Thiele is the archival author.; Keita Ikeda approved the final manuscript. Keita Ikeda attests to the integrity of the original data and the analysis reported in this manuscript.; Hari Osuru approved the final manuscript.; Zhiyi Zuo approved the final manuscript.

decrease in calculated Cyt_{ox} (−0.056 AU, −0.064 to −0.048, $p < 0.001$). The correlations between "discreet" wavelength algorithms (utilizing 4, 6, 8, and 10 wavelengths) and the broadband algorithm for the meausmement of calculated Cyt_{ox} were 0.54 (95% CI 0.52–0.56), 0.87 (0.87–0.88), 0.88 (0.88–0.89), and 0.95 (0.95–0.95), respectively.

Conclusions: the broadband and 10 wavelength algorithm were able to accurately track changes in Cyt_{ox} for all experiments.

Introduction

Near infrared spectroscopy (NIRS) utilizes the modified Beer-Lambert law to estimate the concentration of various biological substances (chromophores) known to absorb near infrared radiation (NIR). The magnitude of NIR absorption by a chromophore can be expressed as optical density (OD) which, according to the modified Beer-Lambert law, is a function of the extinction coefficient of a chromophore (ε), the concentration of the chromophore (c), the path length of the NIR (L), a differential pathlength factor (DPF), and scattering losses.[1] Because ε_λ, L, DPF, and scattering losses are constant, changes in concentration of a chromophore can be described as a function of changing optical densities:

$$\Delta c = \Delta OD_\lambda / (\varepsilon_\lambda \bullet L \bullet DPF)$$

Multiple chromophores can be measured by building a matrix of equations describing c in terms of OD. To solve this matrix at least one wavelength of NIR is needed for each chromophore measured.[2] Clinically, NIRS is commonly used to measure the relative amount of de-oxygenated and oxygenated hemoglobin in tissues (StO_2) such as the brain, which requires at least two wavelengths of NIR.[3]

Hemoglobin is not the only biological compound to absorb NIR. Cytochrome aa_3, the terminal component of the electron transport chain, also absorbs NIR, with a peak around 829 nm.[4] Importantly, the oxidized and reduced forms of cytochrome aa_3 absorb NIR differentially, and thus in theory NIRS can be used to measure the oxidation state of cytochrome aa_3 (Cyt_{ox}) by analyzing additional wavelengths near 829 nm.

The ability of NIRS to measure cyt_{ox} was confirmed using a fluorocarbon exchange model.[5] However, because hemoglobin absorbs NIR more strongly than cytochrome aa_3, and is present in greater quantities, measuring changes in the oxidation state of cytochrome aa_3 in the presence of hemoglobin is technically challenging.[3] Early work on cytochrome NIRS utilized 3–6 wavelength "discrete wavelength" devices, the accuracy of which has been questioned.[2,3] In order to overcome the relatively low stength of the cytochrome aa_3 signal, Matcher et al. developed the "broadband" NIRS technique. Rather than utilizing specific wavelengths of NIR from a laser or light emitting diode (LED) source, broadband NIRS transmits a continuous band of NIR (e.g. 600–900 nm) into tissue using a halogen light source. The strength of the signal returning from the tissue is then measured using a spectrometer, which allows hundreds of wavelengths of light to be measured simultaneously (Figure 1).[2]

There are, however, advantages to using discrete wavelength NIRS devices. Discrete wavelength devices are simpler, less expensive, and most importantly can be adapted to modulate the light source intensity in the megahertz (MHz) range. By measuring the phase shift between emitted and received NIR, phase-modulated NIR devices can measure scattering coefficients and calculate absolute chromophore concentrations.[6]

Broadband and discrete wavelength NIRS algorithms have not been directly compared using a validated model that independently manipulates StO_2 and Cyt_{ox}. To test the accuracy of the broadband device, Cooper et al. developed a staged hypoxia-cyanide injection model which independently alters hemoglobin saturation and Cyt_{ox} (both hypoxia and cyanide lead to Cyt_{ox} reduction, hypoxia leads to a decrease in tissue hemoglobin saturation, where as cyanide leads to an increase in tissue hemoglobin saturation).[7]

The purpose of this study was to compares the performance of broadband and discrete wavelength NIRS algorithms during a staged hypoxia-cyanide injection protocol. We hypothesize that broadband algorithms, but not discrete wavelength algorithms, would accurately measure directional changes in StO_2 and Cyt_{ox} and following staged hypoxia-cyanide administration.

Methods

This study was approved by the institutional animal care and use committee (IACUC) at the University of Virginia.

Animal Model:

All experiments were performed between 7 AM and 5 PM and conducted at a single rodent surgical workstation after at least 48 hours of acclimatization. Ten-week-old male Sprague-Dawley rats from Envigo Corporation (Huntingdon, Cambridgeshire, United Kingdom) weighing approximately 350 g were housed in pairs and individually brought to the workstation, where they were induced with isoflurane and intubated with a 16 gauge catheter using direct visualization. Ventilation was initiated with a SAR-1000 mechanical ventilator (CWE, Inc., Ardmore, PA) and initial settings of 1 Hz respiratory rate, 3.2 mL tidal volume, and 190 mL minute ventilation. End tidal CO_2 ($ETCO_2$) was measured using a microCapStar End-Tidal CO_2 Analyzer (CWE, Inc.) and minute ventilation was adjusted to maintain $ETCO_2$ between 35 and 45 mm Hg. Temperature was measured using a rectal probe (YSI-402, CWE, Inc.) and controlled with a heating pad and TC-1000 Temperature Controller (CWE, Inc.) with a target temperature of 37.0C. Arterial oxygen saturation (SpO_2) was measured with a ML325/BS Oximeter Pod (ADI instruments, Dunedin, New Zealand) taped to the left lower extremity food pad.

Anesthesia was maintained with 1.5% isoflurane in 98.5% oxygen delivered through the EZ-CWE-SA800 Anesthesia System vaporizer (EZ Anesthesia, Palmer, PA). A tail vein was cannulated percutaneously with a 24 gauge intravenous (IV catheter). The right femoral artery was cannulated with a 24 gauge IV catheter using a cut down technique. The arterial cathter was connected to a MLA1052 pressure gauge connected to a FE221 Bridge Amp

(ADI Instruments). All physiological data was recorded and displayed in real time using the PowerLab 8/35 data acquisition system (ADI Instruments)

After instrumentation was complete and physiologic monitoring were established, the temporalis muscles were dissected bilaterally, exposing the skull. A stereotactic frame was then placed directly on the skull so that fiberoptic cables from the halogen light source and spectrometers made direct contact with the parietal bones of the skull.

After achievement of a stable NIRS signal, FiO_2 was decreased to 0.0 until SpO_2 decreased below the measurement limit of 70%, after which FiO_2 was returned to 1.0. One minute later, 5 mg/kg of sodium cyanide (sublethal dose, in order to preserve cardiac output) was injected through the tail vein. This staged process of hypoxia-cyanide injection was repeated every 5 minutes until the animal experienced terminal cardiac arrest (2–3 cycles).

Device Design and Construction:

We constructed a stereotactic frame that positioned the emission and receiving fiberoptic bundles on opposite sides of the rat skull parallel to / on axis with each other. The custom made emission fiber aggregated light from two halogen lamps into a 50um borosilicate bundle, while also providing an SubMiniature version A (SMA) connection to transmit approximately 2% of the source light to a spectrometer so that the source spectrum could be measured in real time (Gulf Photonics, Inc., Oldsmar, FL). QE-Pro piezoelectric cooled charge coupled device (CCD) spectrometers were used for all spectral measurements (Ocean Optics, Dunedin, FL). The QE-Pro utilizes a 10 μm entrance slit, a HC-1 grating with 300–600 lines/mm density, and a 1024×58 element linear silicon CCD array (pixel size: 24 μm × 24 μm, 24 μm pitch]), resulting in a signal-to-noise ratio of 1000:1. Sampling time was individualized based on signal strength but was approximately 4–7 seconds for the received light. The source light was transmitted to the spectrometer using a 200 um 0.22 NA fiberoptic bundle (Thorlabs, Newton, NJ). The receiving light was transmitted to the spectrometer using a 550 um 0.22 NA fiberoptic bundle (Thorlabs). All spectroscopic data was exported to MATLAB (Mathworks, Natick, MA) for off-line analysis.

NIRS Algorithms:

Both spectrometers were calibrated using a standardized light source, and the differences in sensitivities at each wavelength were used to create a transfer function relating each spectrometer to the other. The tissue spectra was adjusted to take into account the differential pathlength factor (DPF), which is wavelength dependent.[8,9] Both the tissue and source spectra were smoothed using a 20 nm window. The intensity of light from the receiving fiberoptic cable opposed to the tissue (I) as well as from the light source (I_0) were converted to absorbance (A) using the following equation:

$$A = -\log_{10}(I/I_0)$$

Chromophore absorbance data for de-oxygenated hemoglobin, oxygenated hemoglobin, and oxidized and reduced cytochrome aa_3 were obtained from the Biomedical Optics Research Laboratory (BORL) at University College, London (UCL).[10] For the discrete wavelength

algorithms, 4–10 wavelengths between 750 and 925 nm were selected. A 4 column matrix (one column for each chromophore) was created, with each row corresponding to the absorption data at each specific wavelength (4–10 rows). Each matrix was pseudoinverted, the result of which was a series of equations describing each chromophore in terms of absorbance at each wavelength of light. For the broadband algorithm, all absorption data from 750–925 nm (1 nm intervals) was entered into the matrix, which was also pseudoinverted to yield a series of equations describing each chromophore in terms of absorbance at each wavelength of light. Details of each algorithm are presented in Table 1.

Absorbance values were entered into the pseudoinverted matrices, the output of which were estimates of de-oxygenated hemoglobin, oxygenated hemoglobin, reduced cytochrome aa_3, and oxidized cytochrome aa_3. Cyt_{ox} was expressed as the "cytochrome difference," the oxidized cytochrome aa_3 minus the reduced cytochrome aa_3 (higher numbers suggest that cytochrome aa_3 is fully oxidized).

Statistical Analysis

We compared changes in Hgb, $HgbO_2$, and Cyt_{ox} after the intial episode of both hypoxia as well as after the initial cyanide injection in each rat. We compared chromophore concentrations at their peak (or trough) before and after (but within 90 seconds of) each intervention. Six comparisons were made – change in Hgb, $HgbO_2$, and Cyt_{ox} after both hypoxia and cyanide injection – thus, a Bonferroni correction was used and a p value of 0.0083 was considered statistically significant. Paired data (i.e. pre-post changes) were tested for normality using the D'Agostino-Pearson normality test, and the paired t-test (parametric) or Wilcoxon Signed rank test (non-parametric) used to compare changes, as appropriate. For correlation analysis of non-independent data (repeated measures from different subjects), inter-subject differences were removed using analysis of covariance.[11] All calculations were performed in MATLAB (Mathworks, Natick, MA), GraphPad Prism 7 (GraphPad Software, La Jolla, CA), and R (R Foundation).

In order to determine whether or not discrete wavelength algorithms might reliably measurement Cyt_{ox}, we compared several discrete wavelength algorithms to broadband algorithms using linear regression technique as well as through graphical analysis.

Previous work by our our group demonstrated that 5 mg/kg cyanide injection led to a change in Cyt_{ox} of −0.0152 arbitrary units (standard deviation 0.0118). We therefore calculated that 20 rats would be needed to have 90% power of detecting a significant change in Cyt_{ox} following cyanide injection. Our primary interest (and outcome) was the ability of NIRS to detect changes in Cyt_{ox} following both hypoxia and cyanide injection.

Results

SpO_2, MAP, $ETCO_2$, and heart rate before and after each intervention are presented in Table 2. Both hypoxia and cyanide injection lead to a decrease in mean arterial blood pressure as well as $ETCO_2$, although the effect of cyanide was more severe. Most notably, cyanide led to a 48% decrease in heart rate (95% CI 41–56%), whereas hypoxia led to a non-significant

increase in heart rate. Arterial lactate after completion of the first stage of hypoxia followed by cyanide averaged 4.2 mEq/L (95% CI 3.6–4.7).

Initiation of hypoxia led to an increase in calculated de-oxyhemoglobin (0.20 arbitrary units [AU] maximal change, 95% CI 0.17 to 0.22, $p < 0.0001$), a decrease in calculated oxy-hemoglobin (−0.16 AU, −0.19 to −0.14, $p < 0.0001$), and a decrease in calculated Cyt_{ox} (−0.057 AU, −0.073 to 0.0040, $p < 0.001$, Figure 2A). Intravenous injection of 5 mg/kg sodium cyanide led to a decrease in calculated de-oxyhemoglobin (−0.037 AU, 95% CI −0.046 to −0.029, $p < 0.001$), an increase in calculated oxy-hemoglobin (0.053 AU, 0.040 to 0.065, $p < 0.001$), and a decrease in calculated Cyt_{ox} (−0.056 AU, −0.064 to −0.048, $p < 0.001$, Figure 2B). Following cardiac arrest, calculated Cyt_{ox} decreased by −0.16 (SD 0.037).

The correlations between “discreet” wavelength algorithms (utilizing 4, 6, 8, and 10 wavelengths) and the broadband algorithm for the meausmement of calculated Cyt_{ox} were 0.54 (95% CI 0.52–0.56), 0.87 (0.87–0.88), 0.88 (0.88–0.89), and 0.95 (0.95–0.95), respectively. A comparison between the 8 and 10 wavelength algorithms and the broadband algorithm are shown in Figure 3. Demonstration of spectral data from one rat is shown in Figure 4.

Discussion

While many clinicians have utilized NIRS principles for the measurement of StO_2, the ability to measure Cyt_{ox} using similar technology is also of interest. In particular, it is known that StO_2, which estimates the supply of oxygen to cells, is subject to artifact such as extracranial contamination.[12,13] In theory, Cyt_{ox}, which measures the energetic state of cells directly, would not be subject to the same artifacts. Animal models of deep hyothermic arrest have found that StO_2 and Cyt_{ox} do not always correlate,[14] and, broadband NIRS has exhibited reductions in Cyt_{ox} despite normal StO_2 following an experimental model of hypoxia and ischemia,[15] all of which suggest that Cyt_{ox} and StO_2 may offer complementary information.

Because the concentration of cytochrome aa_3 is relatively low, and the difference in absorbance between the oxidized and reduced states is relatively week, measurement of Cyt_{ox} is techincally challenging.[3] The realization that discreet wavelength algorithms utilizing up to six wavelengths of NIR performed very differently on three established models of ischemia (rat cerebral hypoxia, piglet cerebral hypoxia, and human forearm ischemia) led some investigators to conclude that early NIRS algorithms were not able to effectively “uncouple” the hemoglobin and cytochrome signals.[3] In response, broadband algorithms were developed and tested using a cyanide injection model. A key feature of the cyanide injection model is the ability of cyanide to initiate both an increase in StO_2 as well as cytochrome aa_3 reduction (decrease in Cyt_{ox}).

Hypoxia is expected to produce hemoglobin desaturation and lead to reduction in cytochrome aa_3. Cyanide injection, by contrast, leads to an *increase* in hemoglobin saturation (because cytochrome aa_3 is inhibited and oxygen cannot be consumed) while also

causing cytochrome reduction. By alternating between hyoxia and cyanide injection in a staged hypoxia-cyanide injection protocol, Cooper et al. were able to confirm the ability of broadband NIRS to independently measure cytochrome aa_3 oxidation state in the presence of hemoglobin.[7] The validity of the broadband NIRS technique was confirmed by Lee at al. who validated a variant of broadband NIRS using a similar staged hypoxia-cyanide injection protocol.[16] We previously reported similar results in a rat model of staged hypoxia-cyanide injection.[17]

It may be possible to develop a discreet wavelength NIRS device that is able to perform similarly to a broadband device. Such a device would be simpler and less expensive than broadband devices, while also allowing for the calculation of absolute chromophore concentrations using frequencey domain techniques. Our analysis suggest that a discrete wavelength device using 10 wavelengths of NIR may be able to reliably trend changes in Cyt_{ox}. Interestingly, our 8 wavelength algorithm was generally able to trend changes in Cyt_{ox}, however for three animals the changes in Cyt_{ox} were exactly the opposite of what would be expected during both hypoxia and cyanide injection. This is likely a reflection of the extremely small signal attributed to changes in the oxidation state of cytochrome aa_3 and therefore the high sensitivity of these algorithsm to any noise or other source of error, which are potentially "averaged out" with increasing numbers of wavelengths. Our 10 wavelength algorithm included an additional wavelength near the cytochrome peak (at 810 nm), and wavelength selection based on chromophore absorption spectral differences may be as important as quantity. Commericially available NIRS devices utilize up to five wavelengths of NIR,[18] and it is not known whether or not ten is technically feasible. If possible, the ability to package 10 wavelengths of light into existing technology would allow for the development of more clinically practical devices capable of measuring absolute chromophore concentrations.

Our study has several limitations. First, like other investigators, we relied on the assumption that sodium cyanide leads to cytochrome aa_3 reduction – there is no available *in vivo* gold standard for the measurement of Cyt_{ox}. *Ex vivo* quantification of cerebral cytochrome activity following injection of cyanide is well-established,[19,20] but real-time quantification of cerebral cytochrome activity in intact tissue remains elusive. Analysis of vital signs (decreasing blood pressure, end-tidal CO_2, and heart rate) as well as elevated lactate levels suggest that injection of sodium cyanide had an adverse effect on subcellular energetics. Second, our algorithm can only measure changes in chromophore concentrations, not absolute values. Third, our "discrete wavelength" algorithm utilized wavelengths taken from a broadband spectrum, which is inefficient. In reality, a dedicated 8 or 10 wavelength device would produce significantly higher signal strength at each individual wavelength (because only discreet wavelengths, as opposed to a large NIR spectrum, would be utilized), and might perform better than the algorithms we tested.

We conclude that broadband NIRS algorithms are capable of measuring directional changes in the oxidation state of cytochrome aa_3 independently of changes in hemoglobin oxygenation, and that discreet wavelength devices including approximately 10 wavelengths, while not commercially available or fully test, may also be able to accurately measure directional changes in the oxidation state of cytochrome aa_3.

Acknowledgements

We would like to thank the Biomedical Optics Research Laboratory (BORL, London, UK) for publishing their chromophore data.

Funding:

Funded by the National Institutes of Health (NIH), 1K08GM115861-01A1 (Thiele)

References

1. Talukdar T, Moore JH, Diamond SG. Continuous correction of differential path length factor in near-infrared spectroscopy. J Biomed Opt. 2013;18(5):56001. [PubMed: 23640027]
2. Matcher SJ, Elwell CE, Cooper CE, Cope M, Delpy DT. Performance comparison of several published tissue near-infrared spectroscopy algorithms. Anal Biochem. 1995;227(1):54–68. [PubMed: 7668392]
3. Ferrari M, Quaresima V. Near infrared brain and muscle oximetry: from the discovery to current applications. Journal of Near Infrared Spectroscopy. 2012;20:1–14.
4. Wray S, Cope M, Delpy DT, Wyatt JS, Reynolds EO. Characterization of the near infrared absorption spectra of cytochrome aa3 and haemoglobin for the non-invasive monitoring of cerebral oxygenation. Biochim Biophys Acta. 1988;933(1):184–192. [PubMed: 2831976]
5. Jobsis FF. Noninvasive, infrared monitoring of cerebral and myocardial oxygen sufficiency and circulatory parameters. Science. 1977;198(4323):1264–1267. [PubMed: 929199]
6. Delpy DT, Cope M. Quantification in tissue near-infrared spectroscopy. *Philosophical Transactions of the Royal Society B*: Biological Sciences. 1997;352:649–659.
7. Cooper CE, Cope M, Springett R, et al. Use of mitochondrial inhibitors to demonstrate that cytochrome oxidase near-infrared spectroscopy can measure mitochondrial dysfunction noninvasively in the brain. J Cereb Blood Flow Metab. 1999;19(1):27–38. [PubMed: 9886352]
8. Kohl M, Nolte C, Heekeren HR, et al. Determination of the wavelength dependence of the differential pathlength factor from near-infrared pulse signals. Phys Med Biol. 1998;43(6):1771–1782. [PubMed: 9651039]
9. Scholkmann F, Wolf M. General equation for the differential pathlength factor of the frontal human head depending on wavelength and age. J Biomed Opt. 2013;18(10):105004. [PubMed: 24121731]
10. London UC. Tissue Spectra. 2005; Absorption spectra data for water, hemoglobin, myoglobin, and cytochromes. Available at: http://www.ucl.ac.uk/medphys/research/borl/intro/spectra. Accessed 03/12/2015, 2015.
11. Bland JM, Altman DG. Calculating correlation coefficients with repeated observations: Part 1--Correlation within subjects. BMJ. 1995;310(6977):446. [PubMed: 7873953]
12. Davie SN, Grocott HP. Impact of extracranial contamination on regional cerebral oxygen saturation: a comparison of three cerebral oximetry technologies. Anesthesiology. 2012;116(4):834–840. [PubMed: 22343469]
13. Greenberg S, Murphy G, Shear T, et al. Extracranial contamination in the INVOS 5100C versus the FORE-SIGHT ELITE cerebral oximeter: a prospective observational crossover study in volunteers. Can J Anaesth. 2016;63(1):24–30. [PubMed: 26307186]
14. Nomura F, Naruse H, duPlessis A, et al. Cerebral oxygenation measured by near infrared spectroscopy during cardiopulmonary bypass and deep hypothermic circulatory arrest in piglets. Pediatr Res. 1996;40(6):790–796. [PubMed: 8947952]
15. Springett RJ, Penrice JM, Amess PN, et al. Non-invasive measurements of mitochondrial damage during neonatal hypoxia-ischaemia--a role for nitric oxide? Biochemical Society transactions. 1997;25(3):398S. [PubMed: 9388628]
16. Lee J, Armstrong J, Kreuter K, Tromberg BJ, Brenner M. Non-invasive in vivo diffuse optical spectroscopy monitoring of cyanide poisoning in a rabbit model. Physiol Meas. 2007;28(9):1057–1066. [PubMed: 17827653]

17. Thiele RH, Ikeda K, Wang Y, Bartz RR, Zuo Z. Broadband near-infrared spectroscopy can detect cyanide-induced cytochrome aa3 inhibition in rats: a proof of concept study. Can J Anaesth. 2017;64(4):376–384. [PubMed: 28008565]

18. Steenhaut K, Lapage K, Bove T, De Hert S, Moerman A. Evaluation of different near-infrared spectroscopy technologies for assessment of tissue oxygen saturation during a vascular occlusion test. J Clin Monit Comput. 2017;31(6):1151–1158. [PubMed: 27878503]

19. Albaum HG, Tepperman J, Bodansky O. The in vivo inactivation by cyanide of brain cytochrome oxidase and its effect on glycolysis and on the high energy phosphorus compounds in brain. J Biol Chem. 1946;164:45–51. [PubMed: 20989467]

20. Albaum HG, Tepperman J, Bodansky O. A spectrophotometric study of the competition of methemoglobin and cytochrome oxidase for cyanide in vitro. J Biol Chem. 1946;163:641–647. [PubMed: 20985634]

Key Points

Question:

can discreet wavelength near infrared spectroscopy (NIRS) algorithm accurately measure changes in the oxidation state of cytochrome aa_3 when manipulated independent of hemoglobin oxygenation?

Findings:

a 10 wavelength NIRS algorithm (but not algorithms using 4, 6, or 8 wavelengths) closely tracked the performance of a broadband NIRS for the meaurement of the oxidation state of cytochrome aa_3 following both hypoxia and cyanide injection.

Meaning:

a 10 wavelength NIRS algorithm may accurately measure directional changes in the oxidation state of cytochrome aa_3, potentially lowering the barrier to producing of a commercially available measurement tool for both scientific and clinical use.

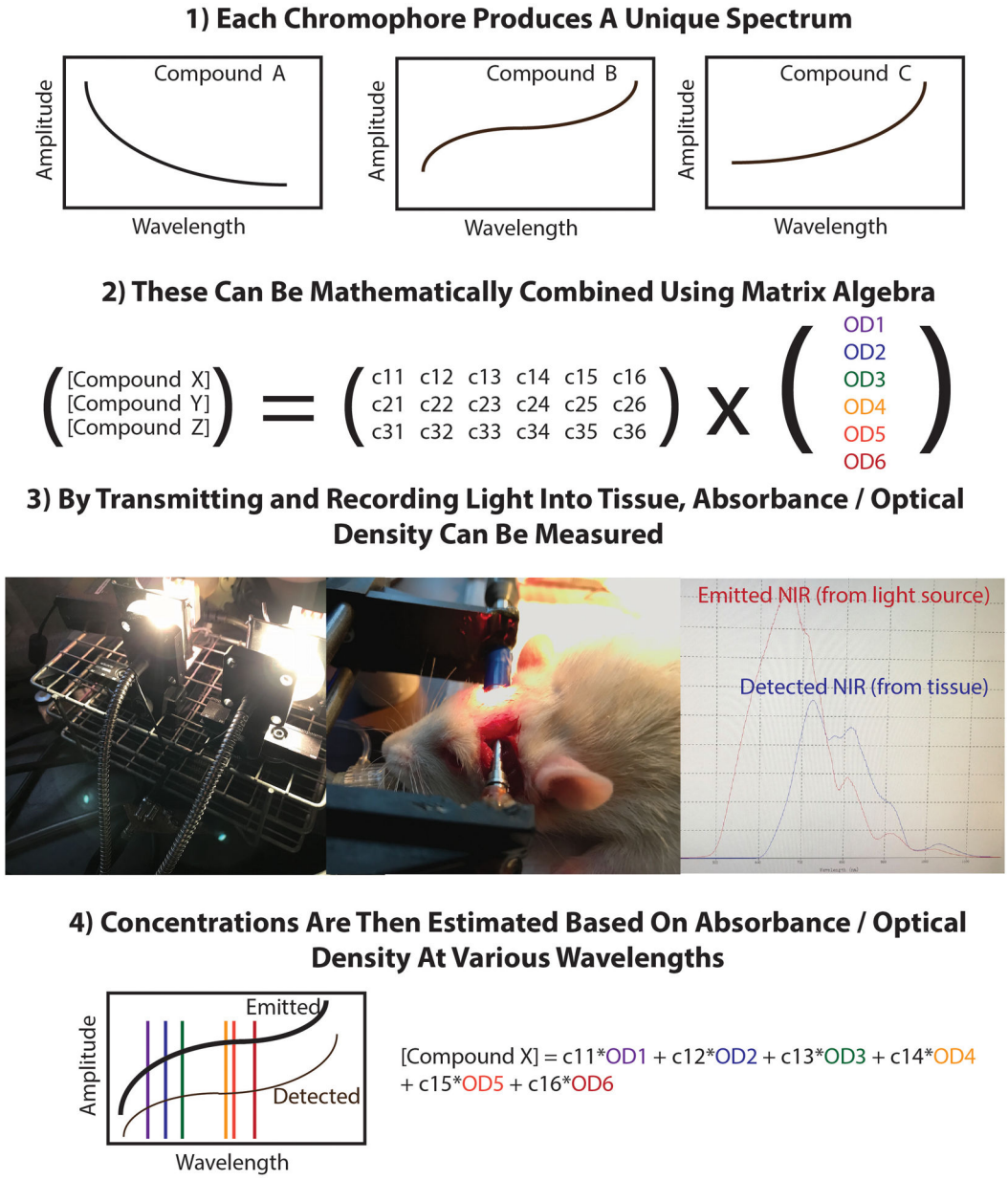

Figure 1.

Schematic of NIRS algorithms. NIR radiation from a dual bulb halogen lamp is emitted into two fiberoptic bundles, one which transmits the signal to a spectrometer which records the intensity of the emitted NIR (**red**), and the other of which transmits NIR to the parietal bone of the rat. The tissue signal (**blue**) is measured on the opposite side of the skull and transmitted to a second spectrometer. All signals are exported to MATLAB for off-line analysis.

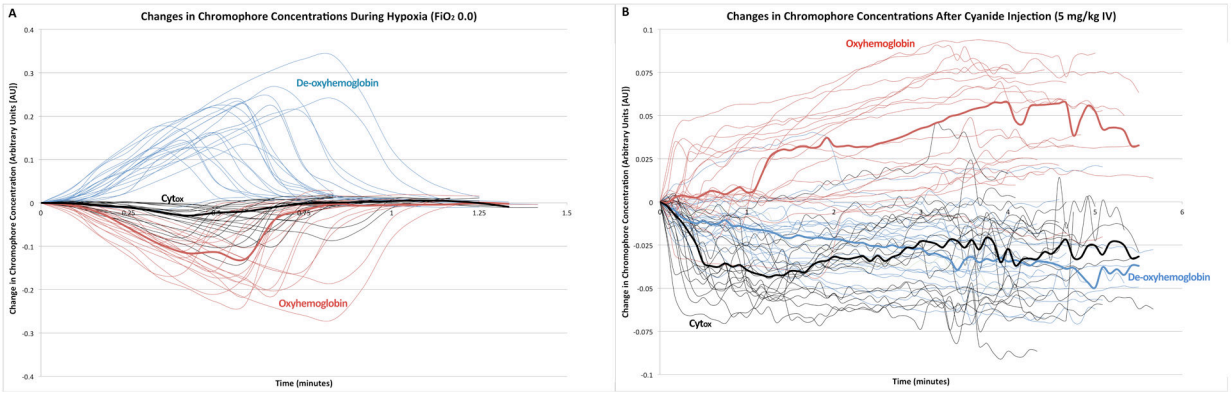

Figure 2.

A) Relative changes in de-oxyhemoglobin (**blue**), oxyhemoglobin (**red**), and cytochrome oxidation state (**black**) for rats after initiation of hypoxia. Median data are presented in bold. B) Relative changes in de-oxyhemoglobin (**blue**), oxyhemoglobin (**red**), and cytochrome oxidation state (**black**) for rats after injection of 5 mg/kg IV NaCN. Median data are presented in bold.

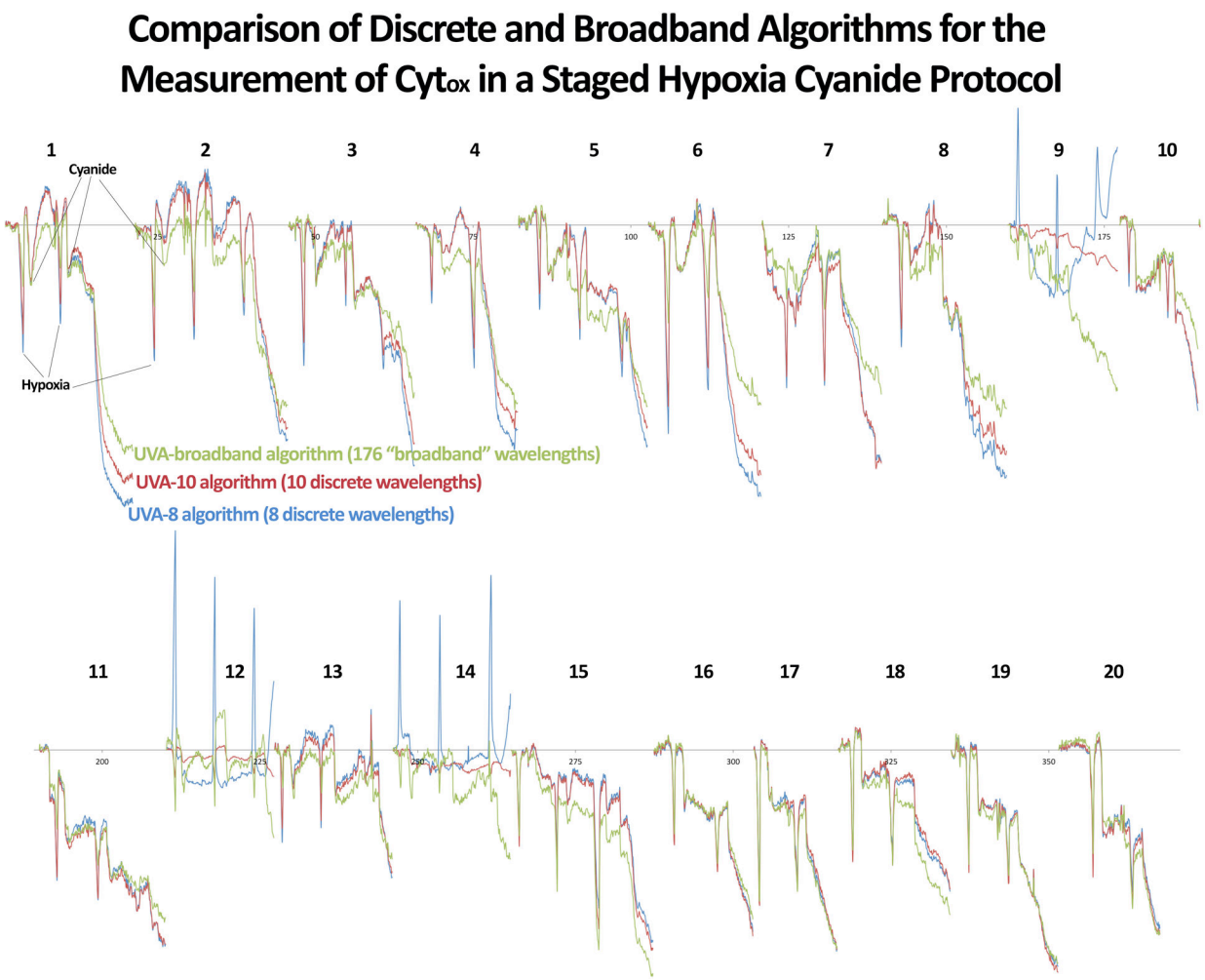

Figure 3.

Comparison of 8 (**blue**) and 10 (**red**) "discreet" wavelength algorithms to the broadband algorithm (**green**) for the measurement of cytochrome aa_3 oxidation state in individual rats.

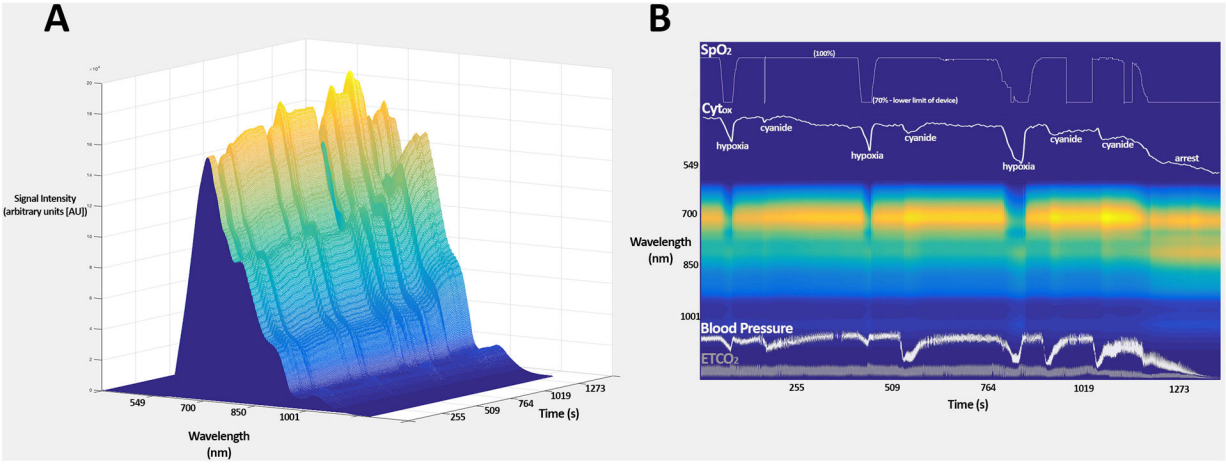

Figure 4.

A) surface plot demonstrating the recorded tissue spectra from rat 15 over time B) compressed spectral array of the recorded tissue spectra from rat 15 over time, with SpO_2, Cyt_{ox} arterial blood pressure, and end-tidal CO_2 overlaid. Note the increased signal at approximately 820 nm (near the cytochrome peak) following injection of cyanide and at the point of cardiac arrest.

Table 1.

Comparison of algorithms utilized. Of note: the peak “cytochrome difference” signal occurs at approximately 829 nm. The blue band includes wavelengths where the cytochrome difference signal is within 95% of the maximal signal at 829 nm.

Algorithm Name	Category	Number of Wavelengths	Wavelengths									
								Cytochrome peak (95%)				
UVA-4	Discrete	4	750		770				820			925
UVA-6	Discrete	6	750	760	770				820		875	925
UVA-8	Discrete	8	750	760	770		790		820	850	875	925
UVA-10	Discrete	10	750	760	770	780	790	810	820	850	875	925
UVA-n	Broadband	176	750–925 nm (1 nm increments)									

Table 2.

Effect of hypoxia and cyanide on hemodynamics. 20 independent measurements (one for each rat) were taken for every variable.

Hypoxia (FiO2 until SpO2 70%)								
Pre/Post	**Pre**	**Post**	**Pre**	**Post**	**Pre**	**Post**	**Pre**	**Post**
Variable	**SpO2 (%)**	**SpO2 (%)**	**MAP (mm Hg)**	**MAP (mm Hg)**	**ETCO2 (mm Hg)**	**ETCO2 (mm Hg)**	**HR (Hz)**	**HR (Hz)**
Value	99.3	70.0	95.1	65.2	45.9	41.3	5.7	5.8
95% CI	98–100	70–70	88–102	58–72	44–47	40–43	5.5–6.0	5.6–6.1
% change		−29 *		−32 *		−10 *		2
95% CI		−30 to −29		−37 to −25		−13 to −7.6		0.23 to 4.1
Cyanide Injection (5 mg/kg NaCN IV)								
Pre/Post	**Pre**	**Post**	**Pre**	**Post**	**Pre**	**Post**	**Pre**	**Post**
Variable	**SpO2 (%)**	**SpO2 (%)**	**MAP (mm Hg)**	**MAP (mm Hg)**	**ETCO2 (mm Hg)**	**ETCO2 (mm Hg)**	**HR (Hz)**	**HR (Hz)**
Value	98.5	97.0	95.1	37.1	45.0	30.0	5.8	3.0
95% CI	97–100	94–100	89–102	32–42	13–47	27–32	5.6–6.1	2.6–3.3
% change		−2		−61 *		−33 *		−48 *
95% CI		−4.7 to 1.7		−65 to −56		−38 to −28		−56 to −41

* Denotes $p < 0.05$